UNCLASSIFIED

DEFENCE RESEARCH ESTABLISHMENT VALCARTIER
CENTRE DE RECHERCHES POUR LA DÉFENSE
VALCARTIER, QUÉBEC

DREV TM - 9615
Limited Distribution / Distribution limitée

ESTIMATION OF AEROSOL MICROPHYSICAL PARAMETERS FROM VISIBLE AND INFRARED EXTINCTION MEASUREMENTS AT MAPTIP

by

D. L. Hutt

July/juillet 1999

Approved by / approuvé par

Gabriel Otten

Section Head/ Chef de section

9 August 99

Date

SANS CLASSIFICATION

WARNING NOTICE

The information contained herein is proprietary to Her Majesty and is provided to the recipient on the understanding that it will be used for information and evaluation purposes only. Any commercial use, including use for manufacture, is prohibited. Release to third parties of this publication or of information contained herein is prohibited without the prior written consent of DND Canada.

© Her Majesty the Queen in Right of Canada as represented by the Minister of National Defence, 1999

105-01798/

ABSTRACT

We show that an effective scattering radius r_s and aerosol extinction coefficient at a wavelength of 3.8 μm, α_e(3.8 μm), can be estimated from the simultaneous measurement of visible and 10.6 μm extinction in haze and fog. For fog, functions relating r_s and α_e(3.8 μm) to the ratio of 10.6 μm to 0.55 μm extinction were derived based on accepted size distribution models for clouds and fog. For haze, functions for r_s and α_e(3.8 μm) were based on an analysis of measured aerosol size distributions. We compare values of r_s and α_e(3.8 μm) derived from measurements of local visible and 10.6 μm aerosol extinction to values obtained from aerosol size spectra at the NATO Panel 4 MAPTIP trial held off the Dutch coast in 1993. We conclude that measurements of visible and 10.6 μm aerosol extinction can provide useful additional information about the aerosols.

RÉSUMÉ

Nous démontrons qu'il est possible de calculer le rayon effectif de diffusion (r_s) et le coefficient d'extinction des aérosols à une longueur d'onde de 3,8 μm, α_e(3,8 μm), en mesurant simultanément le coefficient d'extinction dans le visible et à 10,6 μm dans des conditions de brume et de brouillard. Pour le brouillard, on a obtenu les fonctions de r_s et α_e(3,8 μm) selon le rapport de l'extinction à 10,6 μm et à 0,55 μm, sur la base des modèles de distribution de la taille des aérosols acceptés pour les nuages et le brouillard. Pour la brume, les fonctions r_s et α_e(3,8 μm) étaient basées sur l'analyse des spectres de taille des aérosols mesurés. Nous comparons les valeurs de r_s et α_e(3,8 μm) obtenues grâce aux mesures d'extinction dans le visible et à 10,6 μm à celles obtenues à partir des spectres de taille des aérosols lors de l'essai MAPTIP de la Commission 4 de l'OTAN effectué au large des côtes néerlandaises en 1993. Les mesures d'extinction dans le visible et à 10,6 μm fournissent donc d'autres renseignements utiles sur les aérosols.

TABLE OF CONTENTS

ABSTRACT/RÉSUMÉ i
EXECUTIVE SUMMARY v
1.0 INTRODUCTION 1
2.0 HSS VISIBLE EXTINCTION SENSOR 2
3.0 PVM IR EXTINCTION SENSOR 2
4.0 PMS AEROSOL SPECTROMETERS 3
5.0 FOG AND CLOUD MICROPHYSICAL PARAMETERS 7
6.0 HAZE MICROPHYSICAL PARAMETERS 12
7.0 CONCLUSIONS 17
8.0 ACKNOWLEDGEMENTS 18
9.0 REFERENCES 19
FIGURES 1 to 6
TABLES I and II

EXECUTIVE SUMMARY

Models that predict the performance of electro-optical (EO) systems such as thermal imagers, IR search and track systems (IRST) and laser rangefinders require reliable information about the optical extinction coefficient at the wavelengths of interest. The molecular extinction coefficient can be modelled with great accuracy with computer codes such as LOWTRAN or MODTRAN, using local meteorological conditions as inputs. Unfortunately, extinction due to aerosols varies greatly from one location and time to another, thus accurate and timely information on aerosol extinction must be determined through measurements. Visibility meters that measure the local visible extinction coefficient are widely available but separate measurements of infrared aerosol extinction must be made because visible and infrared aerosol extinction are poorly correlated.

In this paper, we show how simultaneous measurement of visible and 10.6 μm aerosol extinction allow the extinction coefficient at 3.8 μm, α_e(3.8 μm) and the effective scattering radius, r_s, of the aerosol to be deduced. Essentially, measurements of aerosol extinction in the visible and at 10.6 μm characterize the aerosol for wavelengths between approximately 0.55 μm and 12 μm thus providing data than can be used to estimate the performance of any EO system operating from the visible to the far IR. Knowledge of the extinction at 3.8 μm is especially important because it is representative of the 3-5 μm band. Systems operating in the 3-5 μm band experience better angular resolution and less molecular absorption than systems operating in the 8-12 μm band, resulting in better system performance. The CF is currently supporting the development of the SIRIUS dual-band (3-5 and 8-12) IRST. The work described here is already being implemented to validate aerosol models for the SIRIUS project.

Values of r_s and α_e(3.8 μm) derived from measurements of visible and 10.6 μm aerosol extinction are compared to r_s and α_e(3.8 μm) derived from aerosol size spectra measured during the NATO Panel 4 MAPTIP trial held off the Dutch coast in 1993. For fog conditions, it is clear that the technique works well in spite of the fact that little data is available for fog. For haze, the technique is less accurate because the correlation between r_s and α_e(3.8 μm) to the ratio of 10.6 μm to 0.55 μm extinction is poorer than for fog, also the accuracy of the instrument used to measure 10.6 μm extinction is low for haze conditions. Nonetheless, even for haze, measurements of visible and 10.6 μm aerosol extinction allow r_s and α_e(3.8 μm) to be estimated to a useful degree of accuracy.

We conclude that measurements of visible and 10.6 μm aerosol extinction characterize the optical properties of aerosols throughout the visible and infrared bands yielding information relevant to military EO system performance.

1.0 INTRODUCTION

The Marine Aerosol Properties and Thermal Imager Performance (MAPTIP) experiment (Ref. 1) was sponsored by NATO Panel 4 Research Study Groups 5 and 8. MAPTIP took place from 11 October to 5 November 1993, with most of the activities based at the ocean platform Meetpost Noordwijk (MPN) off the Dutch coast at position 45° 16' 25.9'' N, 04° 17' 45.8'' E. One of the goals of the MAPTIP program was to provide aerosol microphysical data for the validation of marine aerosol models.

Extensive measurements of aerosol size distributions were made by several groups with aerosol spectrometers at the MPN platform during the trial. Theoretically, all optical and physical attributes of the aerosol can be derived from the aerosol spectra, although some assumptions about the refractive index have to be made for haze aerosols. However, intercomparison of visible and 10.6 μm extinction coefficient derived from the aerosol spectra measured by the various groups showed that there were difficulties with the calibration and performance of aerosol spectrometers (Ref. 2). Another difficulty with the interpretation of the aerosol spectra is the long integration time required. Under most conditions, integration times of 20 to 30 minutes are required to generate a smooth spectrum.

Direct measurements of aerosol extinction coefficient at 0.55 and 10.6 μm were also made at the MPN platform with forward scatter-type sensors provided by Defence Research Establishment Valcartier (DREV). Calibration and use of these instruments is relatively simple and integration times are only a few seconds so the time evolution of the aerosols can be followed in detail. The drawback of these instruments is that they only provide some of the quantities of interest about the aerosol. However, simultaneous measurements of extinction coefficient at these two widely spaced wavelengths, 0.55 and 10.6 μm does allow other information about the aerosol to be estimated. Here we show how the effective scattering radius and the extinction coefficient at 3.8 μm can be derived from the visible and 10.6 μm extinction measurements and compare them to those derived from the measured aerosol size spectra.

This work was carried out at DREV from May 1993 to December 1995 under PSC 32E15 "EO Battlefield Surveillance/Atmospheric Propagation Studies" and from January to April 1996 under Work Unit 1ab13 "SIRIUS Support".

2.0 HSS VISIBLE EXTINCTION SENSOR

Visible extinction coefficient measurements were made with a model VF-500-110 Visibility Sensor manufactured by HSS Inc., Bedford MA. The sensor measures the visible extinction coefficient by integrating the forward-scattered radiation of a low-divergence light source within an angular range of 39 to 51 degrees (Ref. 3). The source is an infrared emitting diode modulated at 2 kHz. The sample volume is defined by the intersection of the source divergence and the receiver field of view. The sample volume is approximately 400 cm^3. The measurement integration time constant was 10 s. The maximum visible extinction that can be measured by the instrument is 100 km^{-1}. The minimum measurable extinction is determined by the RMS noise of the sensor which is 2 mV for daytime conditions according to the manufacturer. This is equivalent to 0.02 km^{-1}. During the trial, the sensor seemed to meet this specification as the standard deviation of extinction values measured on some of the clearest days was approximately 0.02 to 0.025 km^{-1}. Calibration of the HSS sensor is done by putting a diffusing screen in the sample volume. The scattered signal caused by the diffusing screen represents a visible extinction coefficient of 21.5 km^{-1}, determined through comparison with transmissometer measurements of extinction in natural fog. The accuracy of the HSS sensor for measurement of visible extinction is +/-5%, valid for all types of fog and haze.

3.0 PVM IR EXTINCTION SENSOR

The infrared aerosol extinction coefficient at 10.6 μm, α_e(10.6 μm), was measured with a model PVM-300 particulate volume monitor manufactured by Gerber Scientific Inc., Reston VA. A detailed description of the PVM-300 and the theory of operation and calibration are given in Refs. 4-7. The PVM-300 consists of a collimated laser diode transmitter with a wavelength of 780 nm (just barely within the visible band) and a coaxial receiver located at a distance of 42 cm. The beam irradiates a volume of approximately 3 cm^3. At the center of the receiver is a light trap that intercepts the unscattered beam. Light that is forward scattered from the beam by ambient aerosols passes the light trap and is collected by the receiver in the angular range of approximately 0.3 to 3.6°. At the focal plane of the receiver lens is a circular variable light transmission filter (spatial filter) and just beyond that, a large-area silicon photodiode detector. The spatial filter renders the scattered intensity contributions from aerosols of a given size, proportional to their extinction cross section at a wavelength of 10.6 μm. The total forward scattered signal is thus propor-

tional to the total extinction cross section or the extinction coefficient at 10.6 μm. Thus, a measure of visible light forward scattered by aerosols is transformed into an estimate of the extinction coefficient of those aerosols at 10.6 μm. The extinction coefficient near 10.6 μm has been shown to be approximately proportional to the liquid water content (LWC) of clouds and fog (Ref. 8,9) and a different spatial filter in the instrument yields an output proportional to LWC from which the name particulate volume monitor is derived.

To calibrate the PVM-300 for the measurement of α_e(10.6 μm) the instrument output was compared to aerosol extinction derived from a narrow band transmissometer with peak spectral response at 10.6 μm. The calibration tests were made by the manufacturer in the presence of haze and cloud droplets produced in an environmental chamber. The calibration was transferred to a frosted glass disk which is placed in front of the receiver aperture periodically. The calibration disk scatters a fixed amount of light into the receiver producing a signal equivalent to 9.28 km^{-1} at 10.6 μm. On the basis of the environmental chamber tests, the accuracy of the PVM was determined to be ±10% with a precision of ±0.05 km^{-1}. One of the sources of error for the PVM-300 is that the IR extinction efficiency used to calculate the transmittance profile of the spatial filter depends on the index of refraction of the particles at the wavelength of interest. Since the index of refraction depends on the type and composition of the aerosol the spatial filter was derived for a representative aerosol, the Maritime haze model of Shettle and Fenn (Ref. 10) at a relative humidity of 80%. However, the calibration against the transmissometer, made in the presence of a wide variety of haze and cloud types, shows that the PVM can be used to measure α_e(10.6 μm) for most types of naturally occurring hazes or liquid water clouds.

The PVM and visibility sensors were installed on the MPN platform at a distance of about 3 m from each other. They were fixed to the platform railings at the 15-m level on the north-west corner.

4.0 PMS AEROSOL SPECTROMETERS

The aerosol extinction coefficient depends upon the concentration, size distribution and composition of the aerosol. Direct measurements of these quantities were made on the MPN platform by several groups. Aerosol spectrometers manufactured by Particle Measuring Systems, Boulder CO were used by University of Manchester Institute of

Science and Technology (UMIST), TNO Physics and Electronics Laboratory (TNO) and NRaD (US navy, San Diego). The various instruments were operated independently by each group at different locations on the MPN platform in order to provide complementary information and to address specific objectives. The aerosol spectrometer data is presented and discussed in Ref. 2.

The UMIST aerosol spectrometer equipment consisted of a PMS FSSP-100 covering aerosols in the radius range 0.25 to 23.5 μm and a OAP-230X for ranges 5 to 150 μm. After Oct. 23 these instruments were mounted on the south side of the platform at a height of 7.5 m above mean sea level (amsl). Also a PMS ASASP-X was operated with a heated inlet to provide information on the composition of the accumulation mode particles in the radius range 0.05 to 1.5 μm. The TNO aerosol counter was a PMS CSASP-HV covering the radius range 0.1 to 10 μm. It was mounted on the north-east corner of the MPN platform at a height of 15m amsl. The NRaD system was a PMS ASSP-100 covering the radius range of 0.2 to 15 μm and was mounted at the north-west corner of the platform in a housing that could be lowered down to near the water surface from a height of 15 m amsl.

To compensate for discrepancies between the three sets of aerosol data, to fill in gaps in the individual sets and to take into account the different integration periods of each groups equipment, a set of common aerosol spectra called the consensus data was established and presented in Ref. 2. A fifth order polynomial was fitted to each of the consensus aerosol data sets. Examples of measured aerosols distributions are shown in Figs. 1 a) and b). The polynomials were used to calculate the aerosol extinction coefficient at wavelengths 0.55, 3.8 and 10.6 μm using the Mie computer code from Bohren and Huffman (Ref. 11). The index of refraction was assumed to be that of pure water which is given in Ref. 12 as 1.333-i1.96e-9 at a wavelength of 0.55 μm, 1.364-i0.0034 at 3.8 μm and 1.179-i0.0723 at 10.6 μm. Although droplets smaller than about 1 μm radius are not composed of pure water and thus have indices of refraction different than those given above, those small droplets contribute relatively little to the overall extinction and so the error is expected to be minimal. This supported by the scatter plot of visible extinction coefficients measured by the HSS sensor and calculated from the consensus aerosol data shown in Fig. 2 a). Considering that the aerosol data is typically averaged over 2 hours, the agreement between the visible extinction derived from the aerosol spectra and the sensor (averaged over the same period as the aerosol spectra) is fairly good. This implies that treating the aerosols as pure water is a valid approximation.

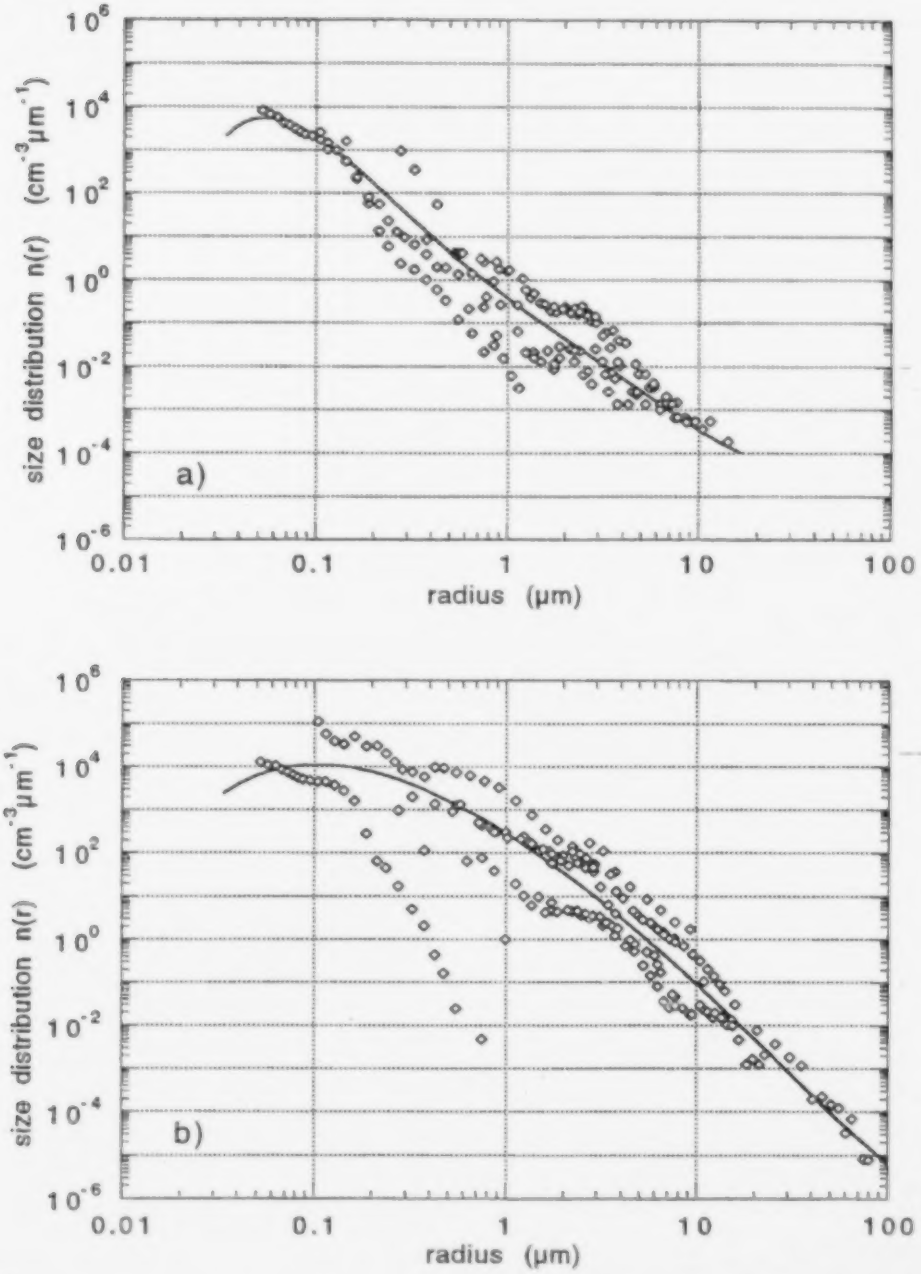

FIGURE 1 - Aerosol spectra from the MAPTIP experiment. a) Haze spectra from 18:00 to 21:00 GMT Oct. 18, 1993, b) Fog spectra measured from 14:15 to 17:15 GMT Oct. 31, 1993

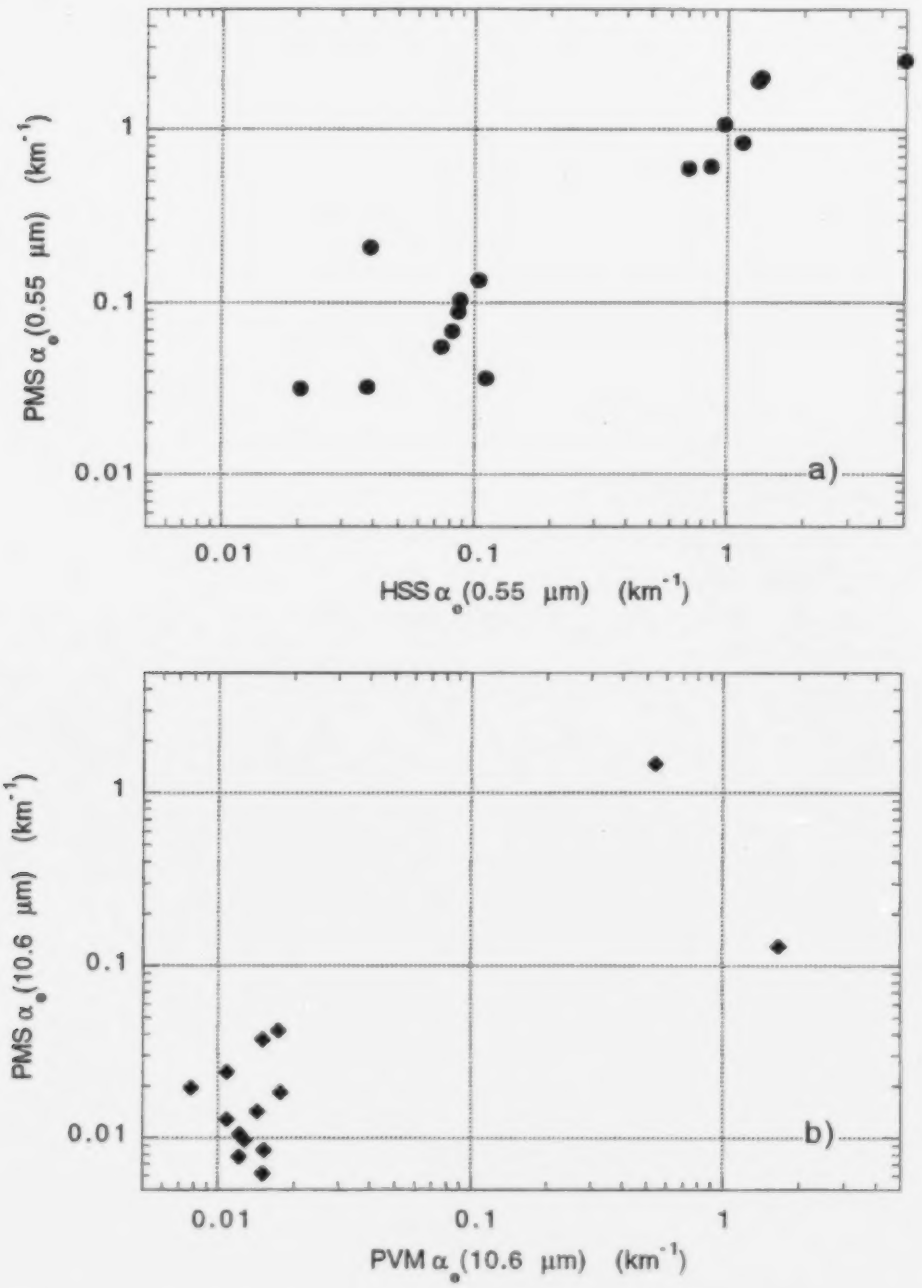

FIGURE 2 - Scatter plots of haze and fog aerosol extinction derived from the consensus MAPTIP aerosol spectra versus that measured with the HSS (a) and PVM (b) probes

The correlation between the extinction coefficient at 10.6 μm derived from the aerosol spectra and the PVM sensor (Fig. 2 b) is not nearly as good as for the visible extinction. The main reason is that the PVM sensor is not sensitive enough to measure aerosol extinction accurately during clear to hazy conditions. Instrument drift can be comparable to the signal being measured. Also, the output of the PVM sensor is more sensitive to the index of refraction of the particles, during clear or hazy conditions when extinction is low and the average size of particles is small. Finally, the extinction at 10.6 μm calculated from the aerosol spectra is more sensitive to truncation error than is the visible extinction. The absence of data for droplets larger than 10 to 16 μm (depending on the data set) can have a significant effect on the calculated 10.6 μm extinction.

5.0 FOG AND CLOUD MICROPHYSICAL PARAMETERS

The size distribution of water droplet fog and clouds is often represented by the modified gamma function:

$$n(r) = Ar^{a}\exp(-br) \ , \qquad (1)$$

where A, a and b are parameters specifying the distribution and r is the droplet radius. Parameters for some accepted models are given in Table I along with optical characteristics calculated using the Mie computer code (Ref. 11) and using the index of refraction of water (Ref. 12). In Table I, N_o is the droplet concentration or the total number of droplets per cm^3 of air.

TABLE I

Characteristics of cloud and fog models

Model	Ref.	A	a	b	N_o (cm^{-1})	r_e (μm)	$\alpha_e(0.55)$ (km^{-1})	$\alpha_e(3.8)$ (km^{-1})	$\alpha_e(10.6)$ (km^{-1})
Adv. fog 1	10	0.0659	3	0.3	20	20.0	31.1	31.0	33.0
Adv. fog 2	10	0.027	3	0.375	20	16.0	18.4	20.2	20.4
Rad. fog	10	607.5	6	3.0	200	3.0	8.65	12.5	1.95
Cumulus 1	13	2.373	6	1.5	100	6.0	16.6	20.5	9.23
Cumulus 2	14	2.604	3	0.5	250	12.0	130.6	146.1	128.8
Stratus	14	27.0	2	0.6	250	8.3	55.1	64.9	41.4
Stratocum.	14	52.73	2	0.75	250	6.67	35.6	43.7	21.7
Altostratus	14	6.268	5	1.11	400	7.21	90.9	107.0	61.3
Nimbostrat.	14	7.676	2	0.425	200	11.5	86.9	97.9	83.2

An effective radius, r_e, of the droplet distribution is defined as

$$r_e = \frac{\int_0^\infty r^3 n(r)dr}{\int_0^\infty r^2 n(r)dr} \quad . \tag{2}$$

For distributions of the form of Eq. 1, r_e may be written,

$$r_e = \frac{a+3}{b} \quad . \tag{3}$$

For water droplet clouds, the extinction coefficient at 10.6 μm is approximately proportional to the third moment of the size distribution (the numerator of Eq. 2) and the visible extinction coefficient is approximately proportional to the second moment (the denominator of Eq. 2) (Ref. 8). Therefore we expect the effective radius of fog or clouds to be a function of the ratio $\alpha_e(10.6\ \mu m)/\alpha_e(0.55\ \mu m)$. Figure 3 a) shows r_e plotted as a function of $\alpha_e(10.6\ \mu m)/\alpha_e(0.55\ \mu m)$ using the data of Table I for the model gamma distributions which are believed to represent a wide range of naturally occurring fog and cloud types. As expected there good correlation between r_e and the extinction ratio. A least squares fit to the data of Fig. 3 a) yields:

$$r_e = 1.79 \exp\left(2.059 \frac{\alpha_e(10.6\mu m)}{\alpha_e(0.55\mu m)}\right) . \tag{4}$$

In Ref. 15, Bissonnette and Hutt showed that there is an approximate functional relationship between the a and b parameters listed in Table I. One possible function relating a and b is:

$$a = -6\left(\frac{1-e^{2.5b}}{1+e^{2.5b}}\right) . \tag{5}$$

Thus an estimate of r_e from Eq. 4 allows both the a and b parameters of the gamma distributions to be determined by solving Eqs. 3 and 5. Knowledge of a, b and $\alpha_e(0.55\ \mu m)$ enables the A parameter to be determined, thus completely specifying the cloud or fog size distribution (Ref. 15).

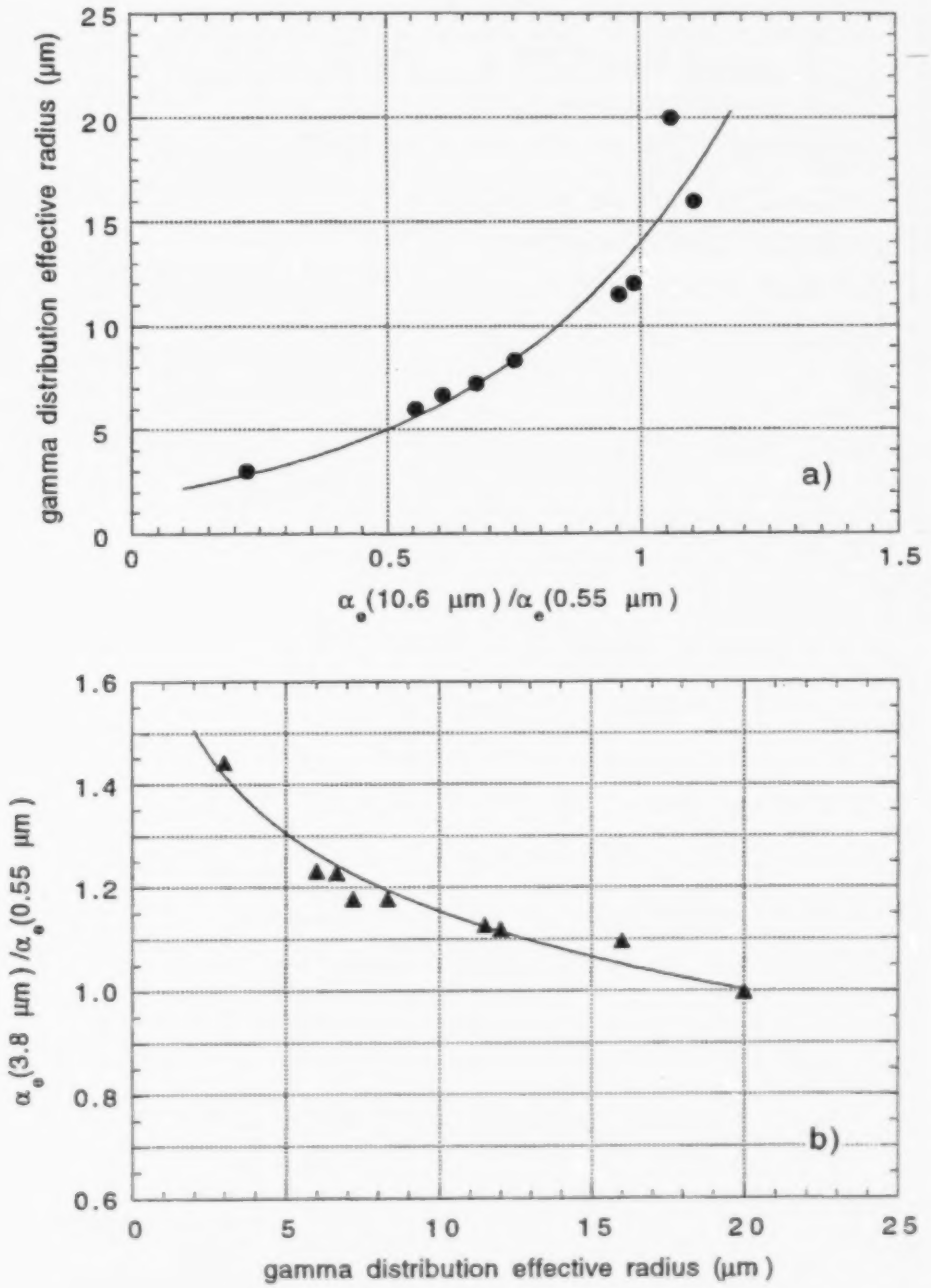

FIGURE 3 - a) Effective radii r_e of gamma distributions from Table 1 plotted as a function of $\alpha_e(10.6\ \mu m)/\alpha_e(0.55\ \mu m)$; b) $\alpha_e(3.8\ \mu m)/\alpha_e(0.55\ \mu m)$ versus r_e

For evaluation of electro-optical system performance, the aerosol extinction coefficient in the 3-5 μm waveband is of particular importance. The extinction at a representative wavelength, 3.8 μm, normalized by the visible extinction coefficient, is well correlated with r_e as shown in Fig. 3 b). A least squares fit to the data of Fig. 3 b) yields

$$\frac{\alpha_e(3.8\mu m)}{\alpha_e(0.55\mu m)} = 1.658 - 0.219\ln(r_e) \quad . \tag{6}$$

Figure 4 a) shows visible and 10.6 μm extinction coefficient measured during the fog episode of Oct. 31 during the MAPTIP experiment. The curves are α_e(0.55 μm) and α_e(10.6 μm) measured by the HSS and PVM sensors, the symbols and horizontal lines represent the one hour average values derived from the UMIST aerosol spectra. The UMIST values for α_e(0.55 μm) and α_e(10.6 μm) are considerably less than those measured by the extinction sensors. This is probably due to reduced efficiency of the UMIST aerosol probes which typically recorded fewer counts than other probes during the trial (Ref. 2). Also, the visible extinction measured with the HSS sensor is in good agreement with estimates of visibility made by an observer on the MPN platform.

Figure 4 b) shows the effective radius and 3.8 μm extinction derived from the extinction sensor data using Eqs. 4 and 6. The effective radius varies from 3 to 6 μm, in good agreement with the UMIST data from 16:00 to 18:00. During this fog episode the wind was easterly, off the land, thus it is unlikely that fog with larger water droplets would be able to form during transport of warm continental air over the short distance of 9 km to the platform. The extinction sensors show that the visible extinction was generally about twice as great as the 10.6 μm extinction, a ratio typical of fog with an effective radius of between 3 and 6 μm. Also, Fig. 4 b) shows that the 3.8 μm extinction derived from the extinction sensor data is slightly greater than the visible extinction which is typical of most fogs and clouds except those with very large r_e where extinction at all visible and IR wavelengths are nearly the same. Both the UMIST data and the extinction sensor data indicate 3.8 μm extinction to be slightly greater than the visible extinction.

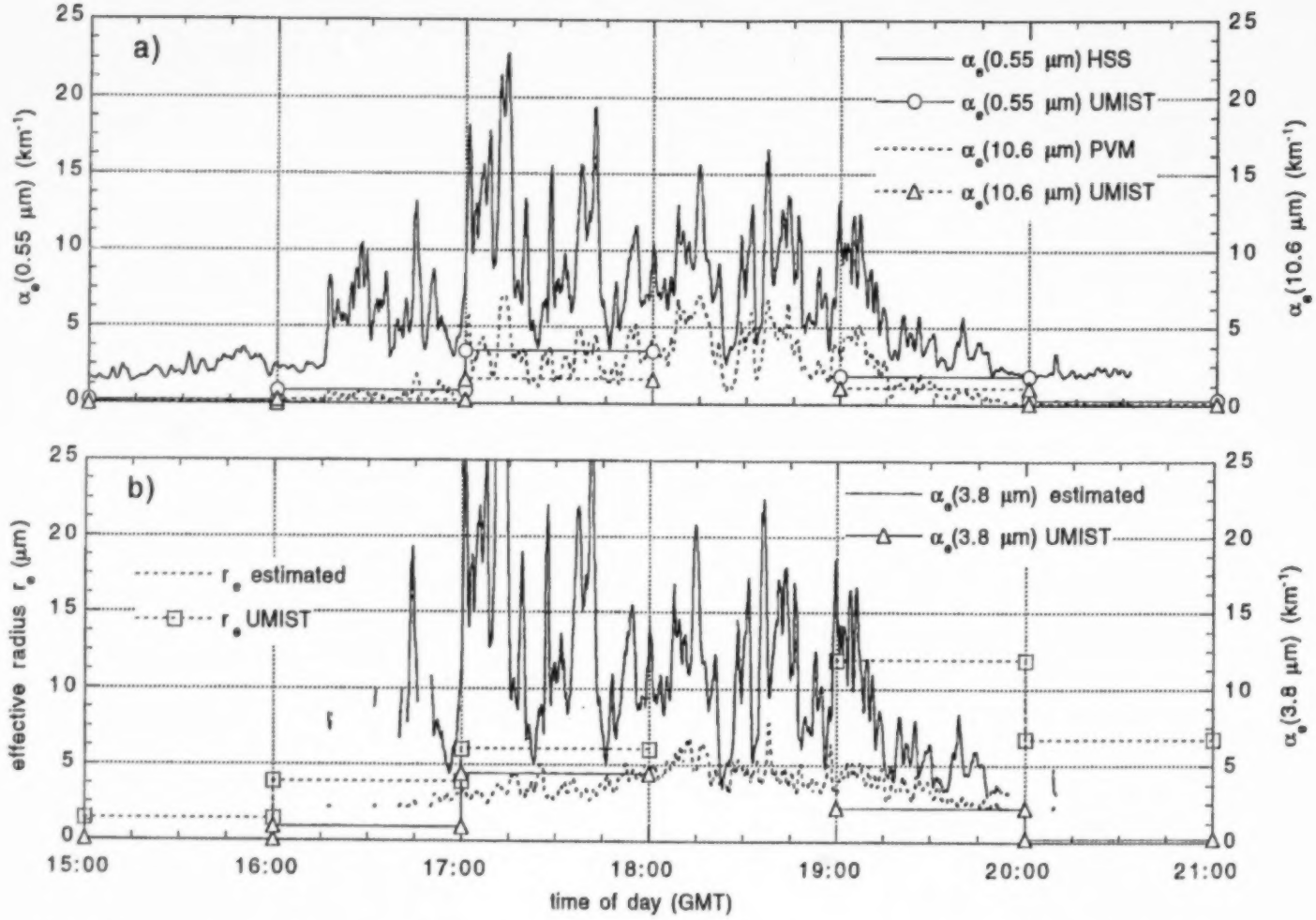

FIGURE 4 - a) α_e(0.55 µm) and α_e(10.6 µm) measured with extinction sensors and derived from the UMIST aerosol spectra for a fog episode on Oct. 31, 1996. b) r_e and α_e(3.8 µm) estimated using Eqs. 4 and 6

The fact that the visible extinction sensor tends to agree with estimates of visibility made by an observer and that the r_e derived from the extinction sensors is relatively small, between 3 and 6 μm supports the validity of the extinction sensor data. Also, it is clear from Fig. 4, that the extinction sensors provided much more data than the 1-hour averages of the aerosol spectrometers. Values for aerosol extinction derived from the consensus aerosol spectra data are in slightly better agreement with the extinction sensors but there are only two measurements available for the period shown in Fig. 4, each averaged for three hours.

6.0 HAZE MICROPHYSICAL PARAMETERS

When the horizontal visibility is between 2 and 20 km, the aerosol type is generally considered to be haze. Often, the sum of two log-normal functions is used to represent the particle size distribution of haze because the modes of the condensation nuclei and hygroscopic components are distinct. Such a bimodal distribution is used by Shettle and Fenn (Ref. 10) to represent rural, urban and maritime aerosols. n(r) for these models is given by,

$$n(r) = \frac{N_1}{rs_1\sqrt{2\pi}}\exp\left\{\frac{[\ln(r)-\ln(r_1)]^2}{2s_1^2}\right\} + \frac{N_2}{rs_2\sqrt{2\pi}}\exp\left\{\frac{[\ln(r)-\ln(r_2)]^2}{2s_2^2}\right\} \qquad (7)$$

where N_i is the total particle concentration for each mode, r_i is the mode radius and s_i is the standard deviation. N_i, r_i and s_i are given in Ref. 10 for rural, urban and maritime type hazes at eight different relative humidities. The values of r_i increase with humidity to represent the growth of the hygroscopic mode with humidity. The rural model is a combination of water soluble and dust-like aerosols, the urban model is a combination of water soluble and soot-like aerosols and the maritime model is a combination of sea salt solution and rural aerosol. Examples of some of the Shettle and Fenn aerosols are given in Table 2 with their optical characteristics. The nominal total particle concentrations are 15000, 20000 and 4000 for the Rural, Urban and Maritime models, respectively.

TABLE II

Characteristics of haze models

Model	RH (%)	N_1	N_2	r_1	r_2	r_e (μm)	$\alpha_e(0.55)$ (km^{-1})	$\alpha_e(3.8)$ (km^{-1})	$\alpha_e(10.6)$ (km^{-1})
Rural	90	0.999875	0.000125	0.039	0.646	0.086	0.341	0.039	0.024
Rural	98	0.999875	0.000125	0.048	0.973	0.139	0.599	0.093	0.052
Rural	99	0.999875	0.000125	0.052	1.176	0.179	0.783	0.136	0.078
Urban	90	0.999875	0.000125	0.042	0.706	0.094	0.556	0.074	0.041
Urban	98	0.999875	0.000125	0.060	1.169	0.163	1.465	0.218	0.116
Urban	99	0.999875	0.000125	0.069	1.486	0.220	2.115	0.352	0.195
Maritime	90	0.99	0.01	0.039	0.380	0.316	0.315	0.203	0.056
Maritime	98	0.99	0.01	0.048	0.602	0.595	0.700	0.593	0.208
Maritime	99	0.99	0.01	0.052	0.751	0.797	1.035	0.954	0.385

Using all 24 Shettle and Fenn haze models, no useful relationship was found between the ratio $\alpha_e(10.6\ \mu m)/\alpha_e(0.55\ \mu m)$ and r_e as was found in the case of the fog and cloud models. However, using the consensus aerosol spectra, a good correlation was found between $\alpha_e(10.6\ \mu m)/\alpha_e(0.55\ \mu m)$ and the effective scattering radius r_s defined as

$$r_s = \frac{\int_0^\infty r\sigma_s n(r)dr}{\int_0^\infty \sigma_s n(r)dr}\ , \tag{8}$$

where σ_s is the scattering cross section. The scattering cross section is the product of the geometrical cross section and the Mie extinction efficiency $Q(r/\lambda)$,

$$\sigma_s = \pi r^2 Q(r/\lambda)\ . \tag{9}$$

The effective scattering radius is representative of the larger particles that contribute most to the extinction in the visible and infrared wave bands. For the fog and cloud distributions at visible wavelengths, the extinction efficiency is close to 2 for most of the droplets and r_s and r_e (Eq. 2) are nearly equal.

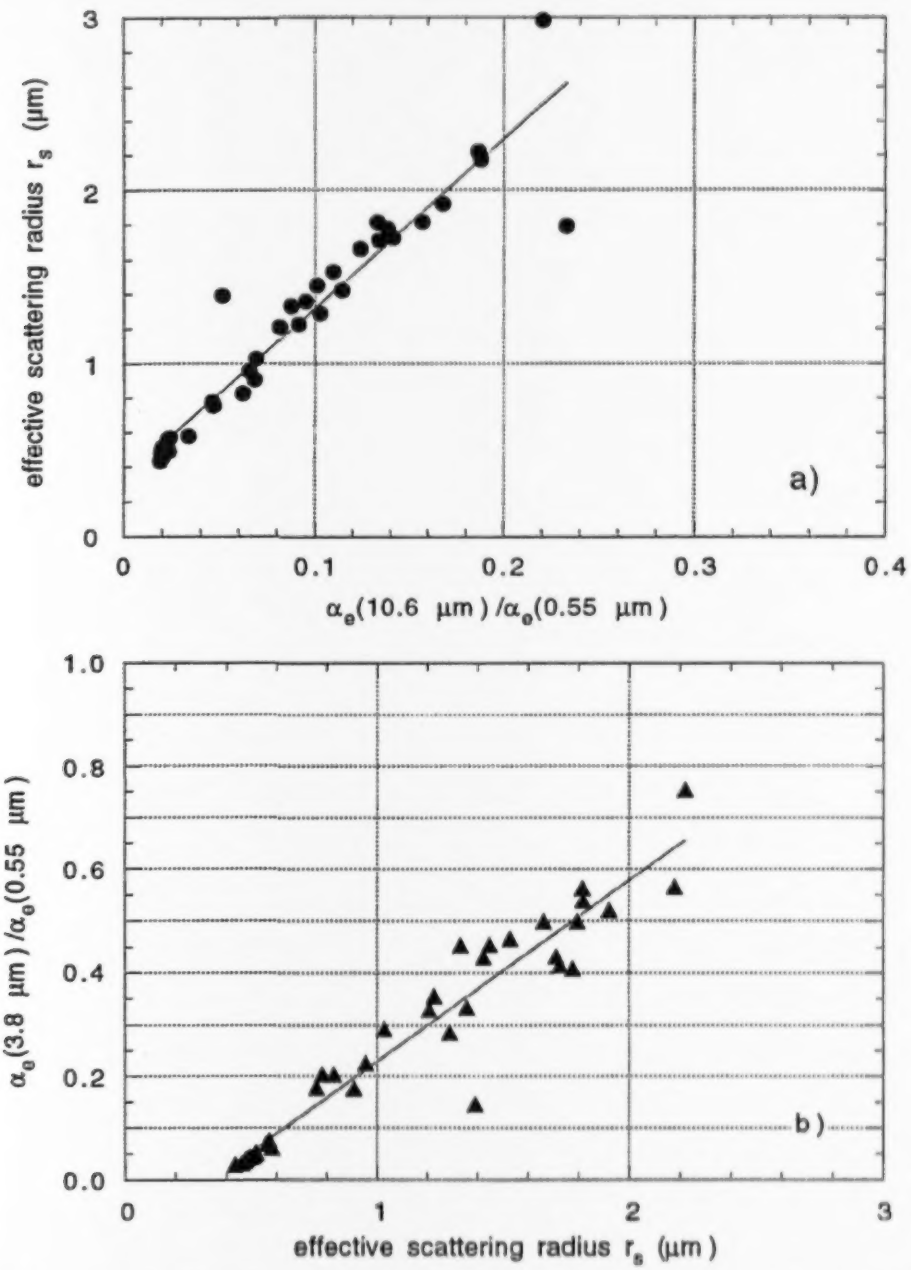

FIGURE 5 - a) Effective scattering radii r_s for the MAPTIP consensus aerosol spectra as a function of α_e(10.6 μm)/α_e(0.55 μm); b) α_e(3.8 μm)/α_e(0.55 μm) as a function of r_s

Evaluating σ_s at a wavelength of 0.55 μm, r_s is plotted as a function of α_e(10.6 μm)/α_e(0.55 μm) in Fig. 5 a). In Fig. 5 b), α_e(3.8 μm)/α_e(0.55 μm) is shown as a function of r_s. Least squares fits to these two plots yield:

$$r_s = 0.34 + 9.78\frac{\alpha_e(10.6\mu m)}{\alpha_e(0.55\mu m)} \tag{10}$$

$$\frac{\alpha_e(3.8\mu m)}{\alpha_e(0.55\mu m)} = -0.121 + 0.349 r_s \quad . \tag{11}$$

Figure 6 shows an example of α_e(0.55 μm) and α_e(10.6 μm) measurements made during one of the many hazy periods encountered during MAPTIP. In this case, α_e(0.55 μm) and α_e(10.6 μm) from the extinction sensors and from the consensus aerosol spectra are in fairly good agreement as are the values of α_e(3.8 μm) and r_s shown in Fig. 6 b). Unfortunately, agreement was usually poor for haze episodes because of the sensitivity limitations of the PVM sensor and the effect of long time averages and truncation error in the aerosol spectra data.

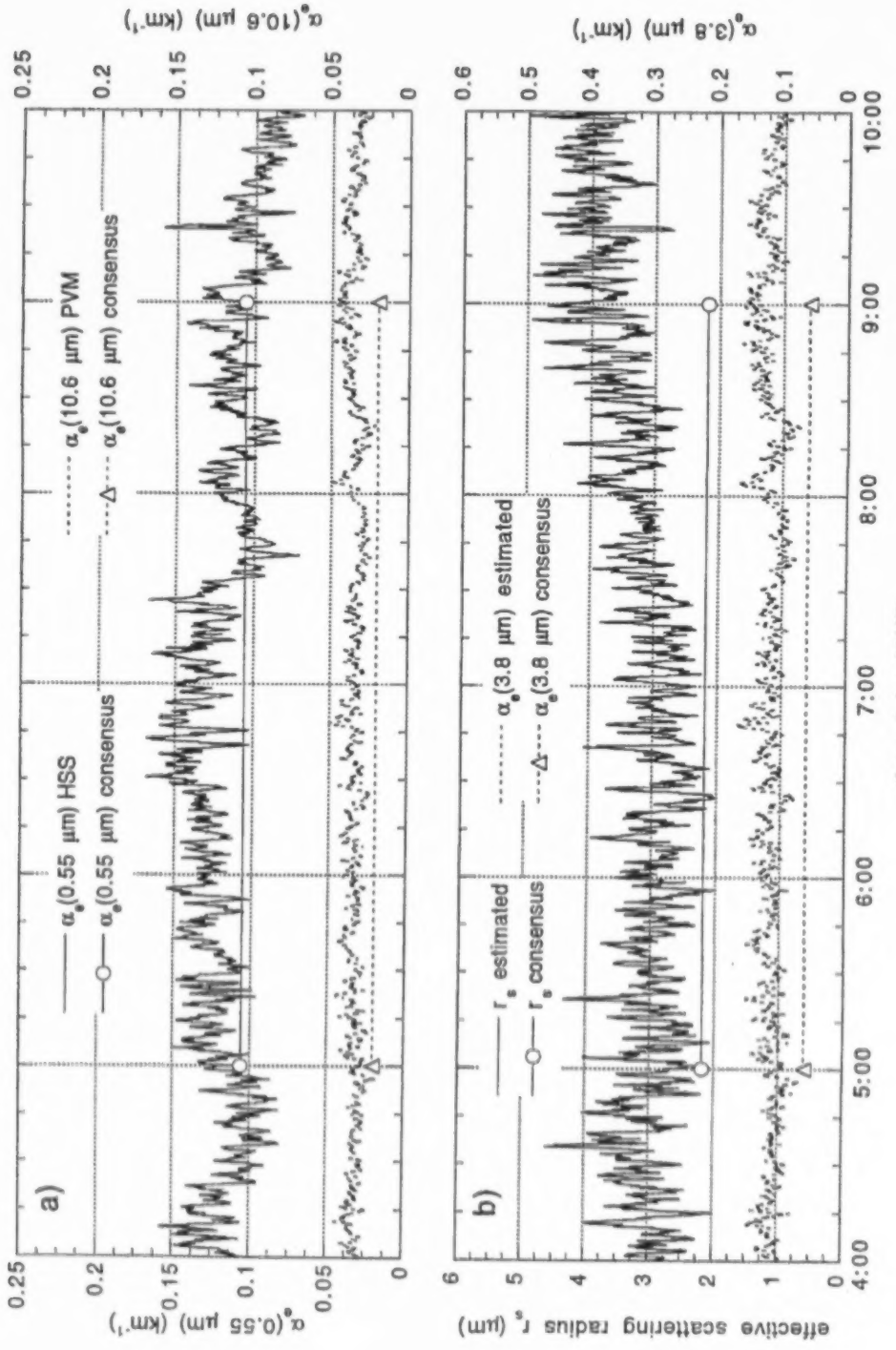

FIGURE 6 - a) α_e(0.55 µm) and α_e(10.6 µm) measured with extinction sensors and derived from the MAPTIP consensus data for haze conditions on Oct. 25, 1993. b) r_e and α_e(3.8 µm) estimated using Eqs. 10 and 11

7.0 CONCLUSIONS

Measurement of aerosol extinction coefficient using forward scatter-type sensors is much easier and has much better time resolution than extinction derived from aerosol size spectra. However, only aerosol spectra provide all the characteristics of the aerosol such as the extinction coefficient at any visible or infrared wavelength, microphysical parameters and the liquid water content. In this paper we showed how two important parameters, an effective scattering radius and the extinction coefficient at 3.8 μm can be derived from measurements of α_e(0.55 μm) and α_e(10.6 μm) made with commercial extinction sensors.

To determine the effective scattering radius and 3.8 μm extinction coefficient, we derived expressions for them in terms of the ratio of α_e(10.6 μm) to α_e(0.55 μm). For fog, the expressions are based on accepted models of fog and cloud droplet size distributions. For haze, the expressions are based on measured aerosol size spectra.

Data collected during the MAPTIP experiment was used to compare values of effective scattering radius and 3.8 μm extinction coefficient derived from measurements of α_e(0.55 μm) and α_e(10.6 μm) to those derived from the aerosol spectra. We found fairly good agreement for the case of fog although the amount of data available for fog was quite limited.

In haze conditions, the PVM infrared extinction sensor was not sensitive enough to provide an accurate measurement of α_e(10.6 μm) and it may have been influenced by variations in the refractive index of the haze. For the aerosol spectrometers, the long time-averaging and the effect of truncation error reduced the accuracy of α_e(10.6 μm) calculated from the aerosol spectra. The combination of these two instrument limitations meant that we were unable to satisfactorily validate the expressions for r_s and α_e(3.8 μm) in haze. Nonethelesss, there were a few cases of haze, such as the one shown in Fig. 6, where r_s and α_e(3.8 μm) derived from the α_e(0.55 μm) and α_e(10.6 μm) measurements were in fairly good agreement with values derived from the aerosol spectrometers. Thus, even for haze there is some indication that the technique works. We hope to better validate it in the future with more detailed data sets and more sensitive instrumentation.

Thus, in spite of the limitations in the MAPTIP data set, estimation of effective scattering radius and 3.8 μm extinction from α_e(0.55 μm) and α_e(10.6 μm) measurements was shown to be a useful technique for fog and possibly for haze as well. The utility of this work will be in long term measurements required to build up statistically meaningful data on aerosol extinction. Such data is necessary for validation of aerosol models and evaluation of the statistics of EO system performance in the marine boundary layer.

8.0 ACKNOWLEDGEMENTS

The author would like to Mr. J. Oman for performing the extinction measurements on the MPN platform and Dr. M. Smith for providing the MAPTIP aerosol spectra.

9.0 REFERENCES

1. G. de Leeuw, A. M. J. van Eijk and D. R. Jensen, "MAPTIP Experiment, Marine Aerosol Properties and Thermal Imager Performance: An overview", TNO report FEL-94-A140, TNO Physics and Electronics Laboratory, The Hague, Netherlands (1994).

2. M. Smith, "Aerosol measurements on the MPN platform during MAPTIP: Is there an aerosol consensus?" University of Manchester, Physics Dept. report, August 1995.

3. J. V. Winstanley and M. J. Adams, "Point visibility meter: a forward scatter instrument for the measurement of aerosol extinction coefficient," Appl. Opt. 14, 2151-2157, 1975.

4. H. Gerber, "Direct measurement of suspended particulate volume concentration and far-infrared extinction coefficient with a laser-diffraction instrument", Appl. Opt. 30,4824-4831 (1991).

5. H. Gerber, "Forward scatter meter for estimating 10.6 μm aerosol extinction", Appl. Opt. 26, 539-544 (1987).

6. H. Gerber, "Infrared aerosol extinction from visible and near-infrared light", Appl. Opt. 24, 4155-4166 (1985).

7. D. L. Hutt, "Aerosol extinction coefficient near 10.6 μm measured with the PVM forward scatter meter and a transmissometer", Proc. SPIE 2471 Atmospheric Propagation and Remote Sensing IV, Orlando, FL, pp. 30-40 (1995).

8. P. Chylek, "Extinction and liquid water content of fogs and clouds", J. Atmos. Sci. 35, 296-300 (1978).

9. R. G. Pinnick, S. G. Jennings, P. Chylek and H. J. Auvermann, "Verification of a linear relation between IR extinction, absorption and liquid water content of fogs", J. Atmos. Sci. 36, 1577-1586 (1979).

10. E. P. Shettle and R. Fenn, "Models for the aerosols of the lower atmosphere and the effects of humidity variations on their optical properties", Air Force Geophysics Laboratory, AFGL-TR-79-0214 (1979).

11. C. F.Bohren and D. R. Huffman, Absorption and Scattering of Light by Small Particles, (John Wiley and Sons, Toronto, 1983), Appendix A, p. 477.

12. G. M. Hale and M. R. Querry, "Optical constants of water in the 200-nm to 200-μm wavelength region", Appl. Opt. 12, 555-563 (1973).

13. D. Dermendjian, "Scattering and polarization properties of water clouds and hazes in the visible and infrared", Appl. Opt. 3, 187-196 (1964).

14. E. P. Shettle, "Models of aerosols, clouds and precipitation for atmospheric propagation studies", Proc. AGARD No. 454, "Atmospheric propagation in the UV, visible, IR and MM-wave region and related system aspects", paper 15 (1989).

15. L. R. Bissonnette and D. L. Hutt, "Multiply scattered aerosol lidar returns: Inversion method and comparison with *in situ* measurements", Appl. Opt. 30 6959-6975 (1995).

INTERNAL DISTRIBUTION

DREV TM-9615

1 - Deputy Director General
1 - Chief Scientist
6 - Document Library
1 - G. Otis
1 - C. Carrier
1 - J.-M. Garneau
1 - D. Dion
1 - L. Bissonnette
1 - G. Roy
1 - J.-M. Thériault
1 - L. Forand
1 - L. Gauthier
1 - M. Duffy

UNCLASSIFIED

EXTERNAL DISTRIBUTION

DREV TM-9615

1 - DRDCIM
1 - DRDCIM (unbound copy)
1 - DRDB
1 - DREA
1 - DREO
1 - DRES
1 - DCIEM
1 - DMSS 6-6-2
1 - DGMetOc/DMWS 2
1 - MARPACHQ/N35 (SSO METOC)
1 - MARLANTHQ/N35

1 - Dr. Dan Hutt (author)
Defence Research Establishment Atlantic
Ocean Acoustics Group
9 Grove Street
Dartmouth, Nova Scotia B2Y 3Z7
Canada

1 - Dr. Douglas R. Jensen
1 - Dr. Kathleen Littfin
1 - Dr. Stu Gathman
NCCOSC RDTE DIV 883
49170 Propagation Path
San Diego CA 92152-7385
USA

1 - Mr. Mike Richards
DERA Portsdown West
C-14, West Court
Portsdown Hill Road
Fareham, Hampshire
UK PO17 6AD

1 - Dr. Jim Gillespie
US Army Research Laboratory
2800 Powder Mill Road, Attn: AMSRL-IS-EE
Adelphi, MD
20783-1197
USA

1 - Dr. G. Kunz
1 - Dr. A. M. J. van Eijk
1 - Dr. G. de Leeuw
Physics Laboratory FEL-TNO
Oude Wallsdorperweg 63
2597 AK, The Hague
The Netherlands

1 - Dr. Mike H. Smith
Physics Deptment UMIST
P.O. Box 88
Manchester
UK M6O 1QD

1 - Mr. Yvonick Hurtaud
CELAR
Division ASRE
35170 Bruz
France

UNCLASSIFIED
SECURITY CLASSIFICATION OF FORM
(highest classification of Title, Abstract, Keywords)

DOCUMENT CONTROL DATA

(Security classification of title, body of abstract and indexing annotation must be entered when the overall document is classified)

1. ORIGINATOR (the name and address of the organization preparing the document. Organizations for whom the document was prepared, e.g. Establishment sponsoring a contractor's report, or tasking agency, are entered in section 8.)
DREV

2. SECURITY CLASSIFICATION (overall security classification of the document including special warning terms if applicable).
UNCLASSIFIED

3. TITLE (the complete document title as indicated on the title page. Its classification should be indicated by the appropriate abbreviation (S,C,R or U) in parentheses after the title).
Estimation of aerosol microphysical parameters from visible and infrared extinction measurements AT MAPTIP

4. AUTHORS (Last name, first name, middle initial. If military, show rank, e.g. Doe, Maj. John E.)
D. L. Hutt

5. DATE OF PUBLICATION (month and year of publication of document)
July 1999

6a. NO .OF PAGES (total containing information Include Annexes, Appendices, etc).
20

6b. NO. OF REFS (total cited in document)
15

7. DESCRIPTIVE NOTES (the category of the document, e.g. technical report, technical note or memorandum. If appropriate, enter the type of report, e.g. interim, progress, summary, annual or final. Give the inclusive dates when a specific reporting period is covered).
TECHNICAL MEMORANDUM

8. SPONSORING ACTIVITY (the name of the department project office or laboratory sponsoring the research and development. Include address).

9a. PROJECT OR GRANT NO. (if appropriate, the applicable research and development project or grant number under which the document was written. Please specify whether project or grant).
1AB11

9b. CONTRACT NO. (if appropriate, the applicable number under which the document was written).

10a ORIGINATOR'S DOCUMENT NUMBER (the official document number by which the document is identified by the originating activity. This number must be unique to this document.)
TM-9615

10b OTHER DOCUMENT NOs. (Any other numbers which may be assigned this document either by the originator or by the sponsor.)
N/A

11. DOCUMENT AVAILABILITY (any limitations on further dissemination of the document, other than those imposed by security classification)
(x) Unlimited distribution
( ) Defence departments and defence contractors; further distribution only as approved
( ) Defence departments and Canadian defence contractors; further distribution only as approved
( ) Government departments and agencies; further distribution only as approved
( ) Defence departments; further distribution only as approved
( ) Other (please specify):

12. DOCUMENT ANNOUNCEMENT (any limitation to the bibliographic announcement of this document. This will normally correspond to the Document Availability (11). However, where further distribution (beyond the audience specified in (11) is possible, a wider announcement audience may be selected).

UNCLASSIFIED
SECURITY CLASSIFICATION OF FORM

13. ABSTRACT (a brief and factual summary of the document. It may also appear elsewhere in the body of the document itself. It is highly desirable that the abstract of classified documents be unclassified. Each paragraph of the abstract shall begin with an indication of the security classification of the information in the paragraph (unless the document itself is unclassified) represented as (S), (C), (R), or (U). It is not necessary to include here abstracts in both official languages unless the text is bilingual).

We show that an effective scattering radius r_s and aerosol extinction coefficient at a wavelength of 3.8 μm, α_e(3.8 μm), can be estimated from the simultaneous measurement of visible and 10.6 μm extinction in haze and fog. For fog, functions relating r_s and α_e(3.8 μm) to the ratio of 10.6 μm to 0.55 μm extinction were derived based on accepted size distribution models for clouds and fog. For haze, functions for r_s and α_e(3.8 μm) were based on an analysis of measured aerosol size distributions. We compare values of r_s and α_e(3.8 μm) derived from measurements of local visible and 10.6 μm aerosol extinction to values obtained from aerosol size spectra at the NATO Panel 4 MAPTIP trial held off the Dutch coast in 1993. We conclude that measurements of visible and 10.6 μm aerosol extinction can provide useful additional information about the aerosols.

14. KEYWORDS, DESCRIPTORS or IDENTIFIERS (technically meaningful terms or short phrases that characterize a document and could be helpful in cataloguing the document. They should be selected so that no security classification is required. Identifiers, such as equipment model designation, trade name, military project code name, geographic location may also be included. If possible keywords should be selected from a published thesaurus, e.g. Thesaurus of Engineering and Scientific Terms (TEST) and that thesaurus-identified. If it not possible to select indexing terms which are Unclassified, the classification of each should be indicated as with the title).

aerosol, aerosol size distribution, scattering coefficient, extinction coefficient, infrared radiation

#511544

DCD03 2/06/87-M/ DREA mod. 17 Dec 1997